THE JOURNAL OF BIOLOGICAL CHEMISTRY VOL. 291, NO. 36, pp. 18947–18958, September 2, 2016
© 2016 by The American Society for Biochemistry and Molecular Biology, Inc. Published in the U.S.A.

Thromboxane A2 Activates YAP/TAZ Protein to Induce Vascular Smooth Muscle Cell Proliferation and Migration*[S]

Received for publication, May 23, 2016, and in revised form, June 30, 2016 Published, JBC Papers in Press, July 5, 2016, DOI 10.1074/jbc.M116.739722

Xu Feng[‡], Peng Liu[‡], Xin Zhou[‡], Meng-Tian Li[‡], Fu-Long Li[‡], Zhen Wang[‡], Zhipeng Meng[§], Yi-Ping Sun[‡], Ying Yu[¶], Yue Xiong[‡‖1], Hai-Xin Yuan[‡2], and Kun-Liang Guan[‡§3]

From the [‡]Key Laboratory of Molecular Medicine of the Ministry of Education and Institutes of Biomedical Sciences, Shanghai Medical College, Fudan University, Shanghai 200032, China, the [§]Department of Pharmacology and Moores Cancer Center, University of California San Diego, La Jolla, California 92130, the [¶]Key Laboratory of Food Safety Research, Chinese Academy of Sciences Center for Excellence in Molecular Cell Science, Institute for Nutritional Sciences, Shanghai Institutes for Biological Sciences, Chinese Academy of Sciences, Shanghai 200031, China, and the [‖]Department of Biochemistry and Biophysics, Lineberger Comprehensive Cancer Center, University of North Carolina, Chapel Hill, North Carolina 27599

The thromboxane A2 receptor (TP) has been implicated in restenosis after vascular injury, which induces vascular smooth muscle cell (VSMC) migration and proliferation. However, the mechanism for this process is largely unknown. In this study, we report that TP signaling induces VSMC migration and proliferation through activating YAP/TAZ, two major downstream effectors of the Hippo signaling pathway. The TP-specific agonists [1S-[1α,2α(Z),3β(1E,3S*),4 α]]-7-[3-[3-hydroxy-4-(4-iodophenoxy)-1-butenyl]-7-oxabicyclo[2.2.1]hept-2-yl]-5-heptenoic acid (I-BOP) and 9,11-dideoxy-9α,11α-methanoepoxy-prosta-5Z,13E-dien-1-oic acid (U-46619) induce YAP/TAZ activation in multiple cell lines, including VSMCs. YAP/TAZ activation induced by I-BOP is blocked by knockout of the receptor *TP* or knockdown of the downstream G proteins $G\alpha_{12/13}$. Moreover, Rho inhibition or actin cytoskeleton disruption prevents I-BOP-induced YAP/TAZ activation. Importantly, TP activation promotes DNA synthesis and cell migration in VSMCs in a manner dependent on YAP/TAZ. Taken together, thromboxane A2 signaling activates YAP/TAZ to promote VSMC migration and proliferation, indicating YAP/TAZ as potential therapeutic targets for cardiovascular diseases.

Thromboxane A2 (TxA2)[4] is produced in many cells/tissues, particularly in platelets (1), and plays an important role in platelet activation and aggregation in vascular injury and atherosclerosis (2). In patients with atherosclerosis or undergoing percutaneous transluminal coronary angioplasty (a non-surgical procedure used to treat the narrowed coronary arteries in cardiovascular disease), the concentration of TxA2 is significantly increased (3–5). A similar phenomenon has also observed in the corresponding mouse models (6–8). TxA2 and thromboxane A2 receptor (TP) are believed to contribute to restenosis after vascular injury (6, 9), which remains a challenging clinical problem, although drug-eluting stents can reduce the risk of restenosis (10).

TxA2 is a type of prostanoid; prostanoids are a family of lipid mediators generated by cyclooxygenase. TxA2 is unstable, with a half-life of about 30 s, and is non-enzymatically degraded into the biologically inactive form thromboxane B2 (TxB2) (1). TxA2 exerts its biological activity through its cognate TP receptor, a G protein-coupled receptor (GPCR) that couples with $G\alpha_{12/13}$, $G\alpha_{q/11}$, and other trimeric G proteins to regulate downstream effectors (11). TP is expressed as two isoforms in humans: TPα and TPβ. Besides TxA2, prostaglandin H2, isoprostanes (such as 8-iso-prostaglandin $F_{2\alpha}$), and hydroxyeicosatetraenoic acids can also activate TP receptors (12–14).

In addition to platelet activation, TxA2 or TP receptor is also known to promote cell migration and proliferation of vascular smooth muscle cells (VSMCs) (15–20), an important process that is involved in a number of vascular diseases, such as post-angioplasty restenosis and atherosclerosis (21). The proliferative response of VSMCs to vascular injury is markedly exaggerated in transgenic mice with vascular overexpression of the human TPα receptor, which can be inhibited by the TP-specific antagonist S18886 (6). Moreover, injury-induced vascular proliferation and platelet activation are suppressed in mice genetically deficient in TP receptor (6). In mouse models of atherosclerosis, both pharmacological antagonism and TP receptor deletion delay lesion development (22–24). Taken together, these previous studies demonstrate that TxA2 and TP receptor contribute to VSMCs mediating vascular disease, although the molecular mechanism is largely unknown.

* This work was supported by National Natural Science Foundation of China Grant 31570784 (to H. X. Y.). K. L. G. is a cofounder of Vivace Therapeutics Inc. The content is solely the responsibility of the authors and does not necessarily represent the official views of the National Institutes of Health.
[S] This article contains supplemental Figs. 1–8.
[1] Supported by National Institutes of Health Grants RO1GM067113, RO1CA068377, and RO1CA163834. To whom correspondence may be addressed: E-mail: yxiong@email.unc.edu.
[2] To whom correspondence may be addressed. E-mail: yuanhaixin@fudan.edu.cn.
[3] Supported by National Institutes of Health Grants R35CA196878, RO1GM51586, and RO1EY022611. To whom correspondence may be addressed. E-mail: kuguan@ucsd.edu.
[4] The abbreviations used are: TxA2, thromboxane A2; TP, thromboxane A2 receptor; GPCR, G protein-coupled receptor; VSMC, vascular smooth muscle cell; CTGF, connective tissue growth factor; MAVSMC, mouse aortic vascular smooth muscle cell; dKO, double knockout; U-46619, 9,11-dideoxy-9α,11α-methanoepoxy-prosta-5Z,13E-dien-1-oic acid; SQ-29548, [1S-[1α,2α(Z),3α,4α]]-7-[3-[[2-[(phenylamino)carbonyl]hydrazino]methyl]-7-oxabicyclo[2.2.1]hept-2-yl]-5-heptenoic acid; I-BOP, [1S-[1α,2α(Z),3β(1E,3S*),4 α]]-7-[3-[3-hydroxy-4-(4-iodophenoxy)-1-butenyl]-7-oxabicyclo[2.2.1]hept-2-yl]-5-heptenoic acid; EdU, 5-ethynyl-2′-deoxyuridine; LATS, large tumor suppressor kinase; MAP4K, mitogen-activated protein kinase kinase kinase kinase; TEAD, TEA domain transcription factor; CRISPR, clustered regularly interspaced short palindromic repeats.

The Hippo signaling pathway plays a key role in the regulation of organ size and tissue homeostasis (25). Core components of the mammalian Hippo pathway include MST1/2 and their adaptor protein SAV1, LATS1/2 and their adaptor proteins MOB1A/1B, and two downstream transcriptional effectors, YAP/TAZ (25). MST1/2 phosphorylate and activate LATS1/2 kinases, which in turn phosphorylate and inhibit YAP/TAZ. Recently, MAP4Ks have been shown to be core components of the Hippo pathway, and they function in parallel to MST1/2 to phosphorylate and activate LATS1/2 (26, 27). Phosphorylation of YAP at Ser-127 results in cytoplasmic sequestration because of 14-3-3 binding (28, 29). The dephosphorylated YAP/TAZ translocate into the nucleus and interact with the TEAD family transcription factors to induce target genes, such as connective tissue growth factor (CTGF) and cysteine-rich angiogenic inducer 61 (CYR61), thereby promoting cell proliferation, migration, and survival (30–32). Deregulation of the Hippo pathway has been observed in various human cancers and is often correlated with a poor prognosis (33). Upstream signals of the Hippo pathway had been elusive until recent studies established that GPCRs relay extracellular signals to the Hippo pathway (34–38). Ligands signaling through GPCRs coupled to $G\alpha_{12/13}$, $G\alpha_{q/11}$, or $G\alpha_{i/o}$ activate YAP/TAZ, whereas ligands signaling through $G\alpha_s$-coupled GPCRs suppress YAP/TAZ activity (36). Therefore, stimulation of different GPCRs can result in either activation or inhibition of YAP/TAZ.

Interestingly, emerging evidence shows that YAP is induced after arterial injury and that its activation promotes smooth muscle phenotypic switching and neointima formation (39, 40). This led us to investigate the function of YAP/TAZ in TxA2- and TP receptor-induced cellular signaling and VSMC migration and proliferation. In this study, we show that TP activation increases YAP/TAZ activity in VSMCs and other cell types via $G\alpha_{12/13}$. Importantly, YAP/TAZ are essential for TP-induced VSMC proliferation and migration, providing a plausible mechanism for VSMC-mediated vascular diseases.

Results

Stimulation of TP Induces YAP/TAZ Dephosphorylation and Nuclear Accumulation—To study TP regulation on YAP/TAZ activity, we treated cells with the TP agonist I-BOP because the physiological TP ligand TxA2 is extremely unstable. In serum-starved HeLa cells that express TP, YAP was highly phosphorylated. Addition of I-BOP resulted in a significant decrease in YAP phosphorylation, as determined by immunoblotting with a phospho-YAP antibody (Ser-127) (Fig. 1, *A* and *B*). I-BOP also induced TAZ dephosphorylation, as indicated by the differential migration on phos-tag gels (Fig. 1*B*). Moreover, I-BOP-induced YAP/TAZ dephosphorylation was rapid and transient, as the YAP/TAZ dephosphorylation was visible 15 min after stimulation and partially recovered 4 h after I-BOP treatment (Fig. 1*B*). In addition, U-46619, another TP-specific agonist, could also induce YAP/TAZ dephosphorylation in a dose- and time-dependent manner (supplemental Fig. 1, *A* and *B*).

Phosphorylation of YAP at Ser-127 by LATS1/2 leads to binding with 14-3-3 and cytoplasmic sequestration of YAP, and dephosphorylated YAP accumulates in the nucleus and induces gene expression by interacting with the transcription factors TEAD1–4 (29, 31). Similarly, phosphorylation of TAZ at Ser-89 by LATS1/2 also induces cytoplasmic localization (30). As expected, I-BOP treatment caused significant nuclear accumulation of YAP and TAZ (Fig. 1, *C* and *D*; supplemental Fig. 1*C*) and enhanced the interaction between YAP and TEAD1 (Fig. 1*E*). A similar effect was also observed when cells were treated with U-46619 (Fig. 1, *C* and *D*; supplemental Fig. 1*C*). To confirm the functional activation of YAP/TAZ upon TP stimulation, we examined the expression of well established YAP/TAZ target genes. The mRNA levels of CTGF and CYR61 were significantly induced by I-BOP or U-46619 treatment (supplemental Fig. 1, *D* and *E*). Accordingly, the CYR61 protein level was also increased upon I-BOP stimulation (Fig. 1*B*).

The effect of TP activation on YAP/TAZ was consistently observed in multiple cell lines, including MDA-MB-231, SW480, and HEK293A (supplemental Fig. 1, *F–I*). Notably, I-BOP also induces YAP/TAZ dephosphorylation in VSMCs, such as the T/G HA-VSMC cell line and primary mouse aortic VSMCs (MAVSMC) (Fig. 1, *F–H*). The effect of I-BOP on YAP/TAZ phosphorylation was dose-dependent, and YAP/TAZ dephosphorylation was evident when as little as 0.1 nmol/liter I-BOP was added to primary MAVSMCs (Fig. 1*H*). Similarly, the expression of YAP/TAZ target genes, such as CTGF, CYR61, TAGLN, and EDN1, was significantly induced by I-BOP in T/G HA-VSMCs (Fig. 1*I*). Based on the above data, we conclude that stimulation of TP activates YAP/TAZ by inducing their dephosphorylation and nuclear translocation.

I-BOP Acts through TP and $G\alpha_{12/13}$ to Activate YAP/TAZ—Because of the unstable property of TxA2, I-BOP and U-46619 were used to treat cells. To exclude that these chemicals have an unexpected effect on YAP/TAZ independent of TP, we pretreated cells with the TP-specific antagonist SQ-29548 followed by I-BOP treatment. As shown in Fig. 2*A*, I-BOP-induced YAP/TAZ dephosphorylation was blocked by SQ-29548 in T/G HA-VSMCs. HEK293A cells are not very sensitive to I-BOP stimulation, likely because of the low level of TP expression. Ectopic expression of TPα receptor rendered YAP/TAZ more sensitive to 1 nmol/liter I-BOP treatment, a concentration that had a minor effect on YAP/TAZ phosphorylation in the control HEK293A cells (Fig. 2*B*). A similar phenomenon was observed when TPβ was overexpressed in U2OS cells (supplemental Fig. 2). These data indicate that I-BOP acts through both isoforms of TP receptor to activate YAP/TAZ.

To further confirm the role of endogenous TP in YAP/TAZ regulation, we generated *TP* KO cells using the CRISPR/Cas9 genome editing system. Two independent *TP* KO cell lines were generated, and the TP deletion was verified by Sanger sequencing (supplemental Fig. 3). *TP* knockout completely blocked I-BOP-induced YAP/TAZ dephosphorylation and YAP nuclear accumulation (Fig. 2, *C* and *D*). Consistently, I-BOP was unable to induce the expression of YAP target genes in *TP* KO cells (Fig. 2*E*). These data show that I-BOP stimulates TP receptor to induce YAP/TAZ activation.

TP receptor activates several trimeric Gα proteins, including $G\alpha_{q/11}$ and $G\alpha_{12/13}$, to initiate intracellular signaling pathways (11). To determine which Gα proteins are involved in YAP/TAZ regulation, $G\alpha_{q/11}$ or $G\alpha_{12/13}$ were knocked down by

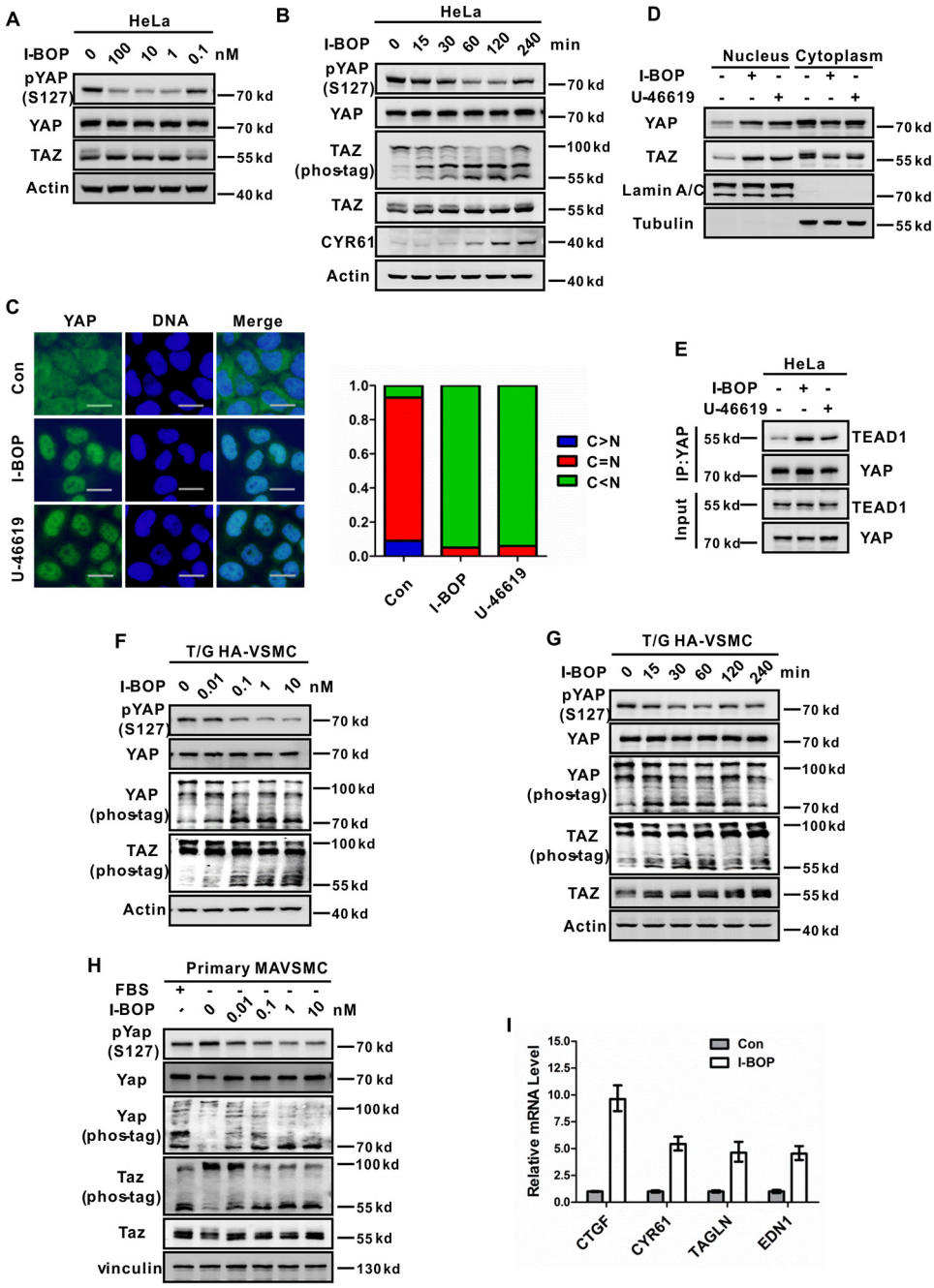

FIGURE 1. **Agonists of TP receptor activate YAP and TAZ.** *A* and *B*, I-BOP induces YAP and TAZ dephosphorylation in a dose- and time-dependent manner in Hela cells. Cells were serum-starved for 16 h and then stimulated with I-BOP for the indicated concentration (*A*) or time (*B*). Immunoblotting was performed with the indicated antibodies. Phos-tag gels were used for assessment of TAZ phosphorylation status. *C*, I-BOP and U-46619 induce YAP nuclear accumulation in HeLa cells. HeLa cells were seeded with a density of 6×10^4 cells/cm^2 for 12 h, starved in serum-free medium for 16 h, and stimulated with 1 nmol/liter I-BOP or 10 nmol/liter U-46619 for 1 h. YAP subcellular localization was determined by immunofluorescence staining for endogenous YAP (*green*). DAPI (*blue*) was used for staining cell nuclei. Representative images are shown. *Scale bars* = 20 μm. Quantifications are shown in the *right panel*. *Con*, control. *D*, I-BOP and U-46619 induce YAP/TAZ nuclear accumulation in HeLa cells. Stimulation conditions were same as those in *C*. Subcellular fractionation was performed with NE-PER^{TM} nuclear and cytoplasmic extraction reagent (Thermo Fisher) according to the instructions of the manufacturer. Both fractions were analyzed by Western blotting with indicated antibodies. *E*, I-BOP and U-46619 enhance YAP interaction with TEAD1. Stimulation conditions were the same as in *C*. Cell lysates were subjected to immunoprecipitation (*IP*) with YAP antibody. The coimmunoprecipitated TEAD1 was detected by immunoblotting. *F* and *G*, I-BOP induces YAP/TAZ dephosphorylation in a dose- and time-dependent manner in T/G HA-VSMCs. Cells were serum-starved for 16 h and then stimulated with I-BOP for the indicated concentration (*F*) or time (*G*). Immunoblotting was performed with the indicated antibodies. Phos-tag gels were used for assessment of YAP/TAZ phosphorylation status. *H*, I-BOP induces Yap/Taz dephosphorylation in a dose-dependent manner in primary MAVSMCs. Cells were serum-starved for 16 h and then stimulated with I-BOP for the concentration as indicated. FBS was included as a positive control. Immunoblotting was performed with the indicated antibodies. Phos-tag gels were used for assessment of Yap and Taz phosphorylation status. *I*, I-BOP induces expression of YAP target genes. T/G HA-VSMCs were treated with 1 nmol/liter I-BOP for 2 h after serum-starved for 16 h. mRNA levels of CTGF, CYR61, TAGLN, and EDN1 were measured by quantitative PCR.

RNAi in HEK293A cells (Fig. 2*F*). Knockdown of $G\alpha_{12/13}$ strongly blocked YAP/TAZ dephosphorylation in response to I-BOP, whereas knockdown of $G\alpha_{q/11}$ had little effect on I-BOP-induced YAP/TAZ dephosphorylation (Fig. 2*F*). Consistently, I-BOP induced YAP nuclear accumulation in control siRNA- and $G\alpha_{q/11}$ siRNA-transfected cells but not in $G\alpha_{12/13}$

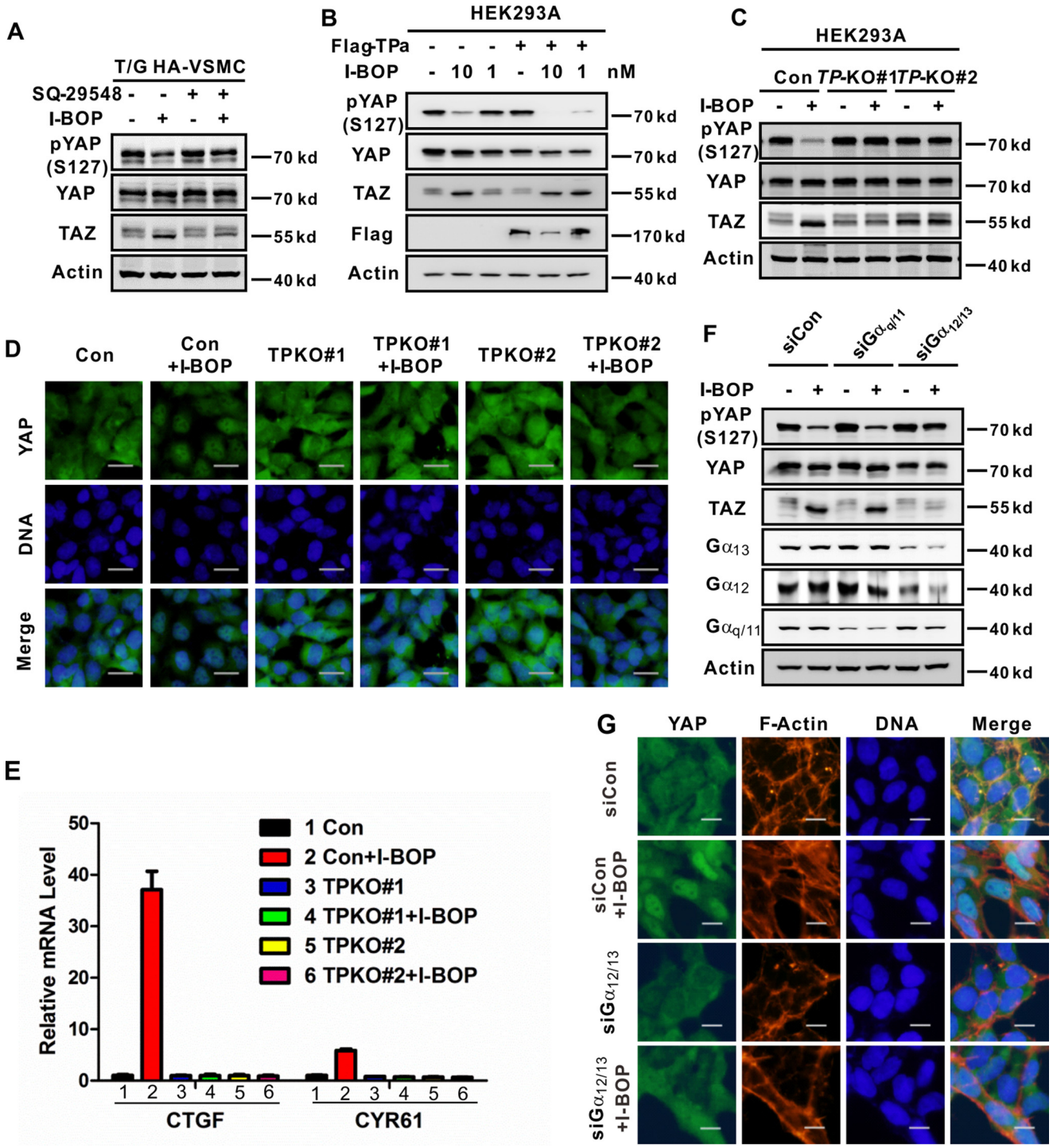

FIGURE 2. **TP agonist activates YAP/TAZ via TP receptor and G$\alpha_{12/13}$.** *A*, the TP antagonist SQ-29548 blocks YAP/TAZ dephosphorylation induced by I-BOP. Serum-starved T/G HA-VSMCs were pretreated with the TP-specific antagonist SQ-29548 (1 μmol/liter) for 3 h and then stimulated with I-BOP (1 nmol/liter) for 1 h. Cell lysates were subjected to immunoblotting with the indicated antibodies. *B*, ectopic expression of TPα receptor renders HEK293A cells sensitive to I-BOP treatment. HEK293A cells were transiently transfected with the indicated plasmids and stimulated with different concentrations of I-BOP for 1 h. Immunoblotting was performed with the indicated antibodies. *C*, knockout of *TP* blocks I-BOP-induced YAP/TAZ dephosphorylation. Wild-type or *TP* KO HEK293A cells, which were verified by genomic DNA sequencing (supplemental Fig. 3), were seeded with a density of 8×10^4 cells/cm^2 for 24 h and then treated with 10 nmol/liter I-BOP for 1 h. Immunoblotting was performed with the indicated antibodies. *Con*, control. *D*, *TP* KO abolishes I-BOP-induced YAP nuclear translocation. Stimulation conditions were the same as in *C*. YAP localization was determined by immunofluorescence. *Scale bars* = 30 μm. *E*, *TP* KO blocks I-BOP-induced target gene expression. Wild-type or *TP* KO HEK293A cells were treated with 10 nmol/liter I-BOP for 2 h. mRNA levels of CTGF and CYR61 were measured by quantitative PCR. *F*, I-BOP activates YAP/TAZ via G$\alpha_{12/13}$. HEK293A cells were transfected with the indicated siRNAs. A mixture of two independent oligonucleotides was used for one gene. Two days after transfection, cells were treated with 10 nmol/liter I-BOP for 1 h. cells were lysed and subjected to immunoblotting with the indicated antibodies. *G*, knockdown of G$\alpha_{12/13}$ blocks I-BOP-induced YAP nuclear localization. Stimulation conditions were similar as in *F*. Immunofluorescence staining for endogenous YAP (*green*), F-actin (*red*), and DNA (*blue*) is presented. *Scale bars* = 20 μm.

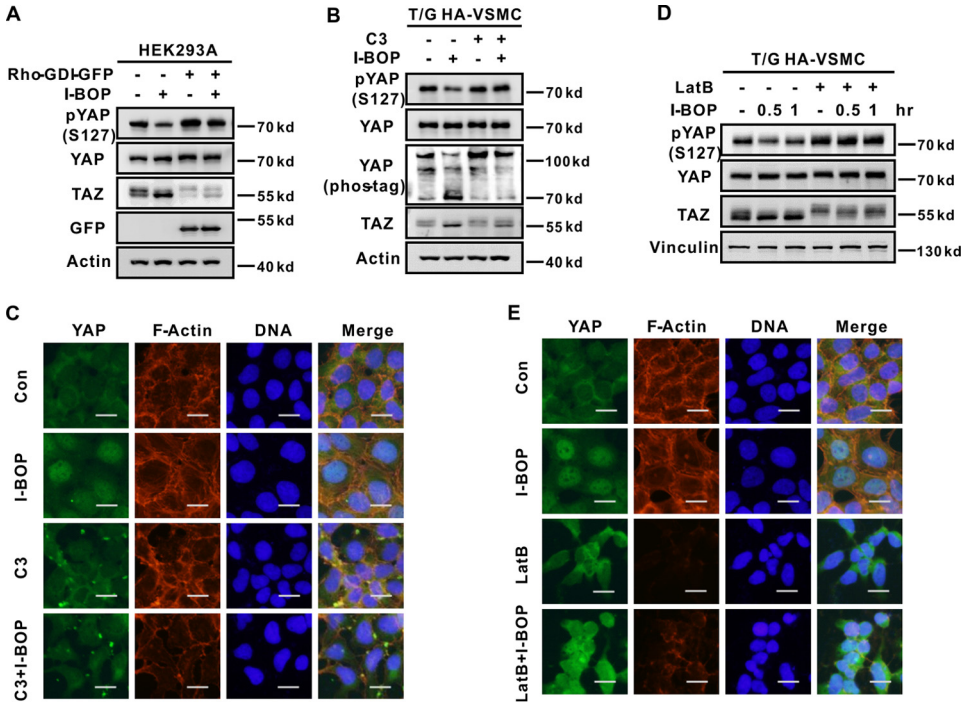

FIGURE 3. **I-BOP activates YAP/TAZ through Rho and cytoskeletons.** *A*, I-BOP-induced YAP/TAZ dephosphorylation is blocked by Rho-GDP dissociation inhibitor expression. HEK293A cells were transiently transfected with the indicated plasmids and incubated with 10 nmol/liter I-BOP for 1 h. Immunoblotting was performed with the indicated antibodies. *B*, inactivation of Rho by C3 prevents YAP/TAZ dephosphorylation. Serum-starved T/G HA-VSMCs were pretreated with C3 (4 μg/ml) for 3 h and then stimulated with I-BOP (1 nmol/liter) for 1 h. The cell lysates were subjected to immunoblotting analysis with the indicated antibodies. *C*, inactivation of Rho by C3 prevents YAP nuclear accumulation. Serum-starved HEK293A cells were pretreated with C3 (2 μg/ml) for 3 h and then stimulated with I-BOP (10 nmol/liter) for 1 h. After fixation, immunofluorescence staining was performed for endogenous YAP (*green*) and F-actin (*red*). DAPI (*blue*) was used for staining cell nuclei. *Scale bars* = 20 μm. *Con*, control. *D*, disruption of the actin cytoskeleton blocks I-BOP-induced YAP/TAZ dephosphorylation. Serum-starved T/G HA-VSMCs were pretreated with Latrunculin B (*LatB*, 1 μg/ml) for 10 min and then stimulated with I-BOP (1 nmol/liter) for the indicated time. The cell lysates were subjected to immunoblotting analysis with the indicated antibodies. *E*, disruption of the actin cytoskeleton blocks I-BOP-induced YAP nuclear localization. HEK293A cells were pretreated with Latrunculin B (1 μg/ml) for 10 min and then stimulated with I-BOP (10 nmol/liter) for 1 h. The immunofluorescence staining is similar as in *C*. *Scale bars* = 20 μm.

siRNA-transfected cells (Fig. 2*G*, supplemental Fig. 4). Taken together, we conclude that TP signals through $G\alpha_{12/13}$ to induce YAP/TAZ dephosphorylation and activation.

I-BOP Modulates YAP/TAZ Dephosphorylation via Rho GTPase and the Actin Cytoskeleton—Rho GTPase is a known downstream signaling module of $G\alpha_{12/13}$, which directly interacts and activates the Rho guanine nucleotide exchange factor. We therefore tested the role of Rho GTPase in I-BOP-induced YAP/TAZ dephosphorylation. Expression of Rho GDP dissociation inhibitor, which binds to Rho GTPase and inhibits GTPase cycling, suppressed I-BOP-induced YAP/TAZ dephosphorylation (Fig. 3*A*). Likewise, botulinum toxin C3, a specific inhibitor of Rho GTPase, strongly blocked YAP/TAZ dephosphorylation in response to I-BOP or U-46619 treatment (Fig. 3*B*; supplemental Fig. 5, *A* and *B*). Consistently, C3 treatment blocked I-BOP- or U-46619-induced YAP nuclear translocation (Fig. 3*C*, supplemental Fig. 5*C*). These data indicate that Rho GTPase is required for TP to activate YAP/TAZ.

The major function of Rho GTPase is to modulate the actin cytoskeleton, particularly stress fiber formation. Recently studies have shown that the actin cytoskeleton plays an important role in the Hippo pathway (41–45). We therefore tested whether cytoskeletal reorganization contributes to YAP/TAZ activation by TP agonists. Latrunculin B, an F-actin-disrupting reagent, blocked I-BOP- or U-46619-induced YAP/TAZ dephosphorylation (Fig. 3*D*, supplemental Fig. 5*D*). Consistent with changes in YAP phosphorylation, Latrunculin B treatment also prevented YAP nuclear accumulation in response to I-BOP or U-46619 (Fig. 3*E*, supplemental Fig. 5*E*). Moreover, I-BOP or U-46619 induced actin stress fiber and YAP nuclear translocation (Figs. 2*G* and 3, *C* and *E*; supplemental Fig. 5, *C* and *E*). Knockdown of $G\alpha_{12/13}$ or treatment with C3 or Latrunculin B disrupted F-actin formation and YAP nuclear accumulation (Figs. 2*G* and 3, *C* and *E*; supplemental Fig. 5, *C* and *E*). These results indicate that TP acts through Rho GTPase and the actin cytoskeleton to affect YAP/TAZ phosphorylation.

I-BOP Inhibits LATS—LATS1/2 are the kinases directly responsible for YAP/TAZ phosphorylation. The phosphorylation of the activation loop (Ser-909/Ser-872 for LATS1/2) and hydrophobic motif (Thr-1079/Thr-1041 for LATS1/2) correlates with LATS1/2 kinase activity (46). To test whether LATS1/2 kinases are involved in I-BOP-induced YAP/TAZ activation, we measured LATS1 kinase activity *in vitro*. LATS1 was potently inhibited by I-BOP treatment, as determined by its autophosphorylation at Ser-909 and *in vitro* phosphorylation of the purified GST-YAP (Fig. 4*A*). Consistent with the results described in Fig. 3, *B* and *C*, inhibition of Rho GTPase by C3 blocked the inhibitory effect of I-BOP on LATS1 kinase activity (Fig. 4*A*), indicating that Rho GTPase activation is required for I-BOP-induced LATS1 inhibition. To further determine the role of LATS1/2 in YAP regulation by I-BOP, we used *LATS1/2* double knockout (LATS1/2 dKO) HEK293A cells. As expected,

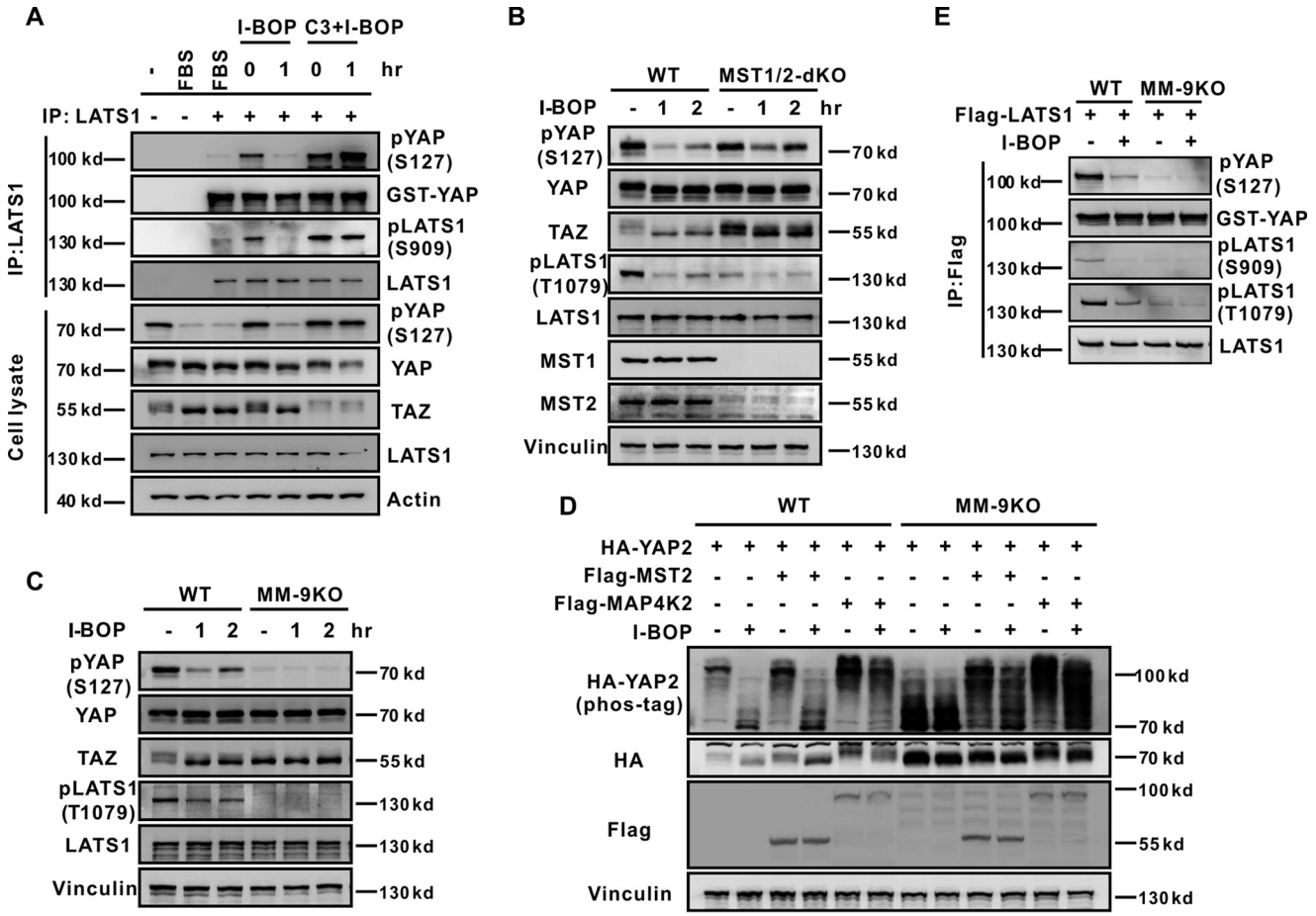

FIGURE 4. **I-BOP inhibits LATS.** *A*, I-BOP inhibits the activation loop phosphorylation of LATS1 in a Rho-dependent manner. HEK293A cells were pretreated with C3 (2 μg/ml) for 3 h and then stimulated with I-BOP (10 nmol/liter) for 1 h. The presence of FBS is indicated. Cell lysates were subjected to immunoprecipitation (*IP*) with control IgG or LATS1 antibody. The immunoprecipitated LATS1 was measured for the *in vitro* kinase assays using GST-YAP as a substrate. The phosphorylation of LATS1 and GST-YAP was detected by immunoblotting with the indicated antibodies. *B*, MST1/2 are not essential for I-BOP-induced YAP/TAZ dephosphorylation. Wild-type or MST1/2 dKO HEK293A cells were treated with I-BOP (10 nmol/liter) for the indicated time points. The cell lysates were subjected to immunoblotting with the indicated antibodies. *C*, both MST1/2 and MAP4Ks are involved in I-BOP-induced YAP/TAZ dephosphorylation. Wild-type or MM-9KO HEK293A cells, which were verified by genomic DNA sequencing (supplemental Fig. 7), were treated with I-BOP (10 nmol/liter) for the indicated time. The cell lysates were subjected to immunoblotting as indicated. D, re-expression of MST1/2 or MAP4K2 in MM-9KO cells restores I-BOP-induced YAP/TAZ dephosphorylation. Wild-type or MM-9KO HEK293A cells were transfected with the indicated plasmids and treated with I-BOP (10 nmol/liter) for 1 h. The cell lysates were subjected to immunoblotting as indicated. *E*, MST1/2 and MAP4Ks are required for I-BOP to induce LATS inhibition. Wild-type or MM-9KO HEK293A cells were transfected with the indicated plasmids and treated with I-BOP (10 nmol/liter) for 1 h. The Cell lysates were subjected to immunoprecipitation with FLAG beads. The immunoprecipitated FLAG-LATS1 was measured for *in vitro* kinase assays using GST-YAP as a substrate. The phosphorylation of LATS1 and GST-YAP was detected by immunoblotting with the indicated antibodies.

I-BOP could not affect YAP/TAZ phosphorylation in LATS1/2-dKO cells (supplemental Fig. 6), suggesting that LATS1/2 are required for I-BOP-induced YAP/TAZ dephosphorylation.

MST1/2 and MAP4Ks are responsible for LATS kinase activation in response to upstream signals (26, 27, 46). To test whether MST1/2 or MAP4Ks are involved in I-BOP-induced YAP/TAZ dephosphorylation, we used *MST1/2* double knockout (MST1/2 dKO) and combined deletion of *MST1/2* and *MAP4K1/2/3/4/5/6/7* (MM-9KO) HEK293A cells (supplemental Fig. 7). I-BOP-induced YAP/TAZ dephosphorylation was largely unaffected in MST1/2 dKO cells (Fig. 4*B*). However, I-BOP had no effect on YAP/TAZ phosphorylation in MM-9KO cells (Fig. 4*C*). In addition, re-expression of MST2 or MAP4K2 could restore the effect of I-BOP on YAP phosphorylation in MM-9KO cells (Fig. 4*D*). I-BOP-induced LATS inhibition was abolished in MM-9KO cells, as shown by *in vitro* kinase assay (Fig. 4*E*). Taken together, these results suggest that MAP4Ks play a major role in I-BOP-induced YAP/TAZ dephosphorylation, although both MST1/2 and MAP4Ks are involved.

YAP/TAZ Are Required for TP to Stimulate VSMC DNA Synthesis and Cell Migration—TP has been shown to promote neointima formation, which is caused by VSMC migration and proliferation (6, 9, 47). Because YAP/TAZ activity is significantly activated upon TP stimulation in VSMCs, we investigated whether YAP/TAZ activation is involved in the proliferation and migration of VSMCs. *YAP/TAZ* were knocked down in T/G HA-VSMCs by inducible shRNA and siRNA, respectively. The knockdown efficiency was confirmed by immunoblotting of protein levels (Fig. 5*A*). Knockdown of *YAP/TAZ* significantly suppressed the mRNA induction of CTGF and CYR61 in response to I-BOP (Fig. 5*B*). I-BOP strongly induced cell migration in control cells, whereas this effect was significantly suppressed in *YAP/TAZ* double knockdown cells (Fig. 5, *C* and *D*). In addition, I-BOP-induced VSMC DNA synthesis was also suppressed by *YAP/TAZ* double knockdown, as deter-

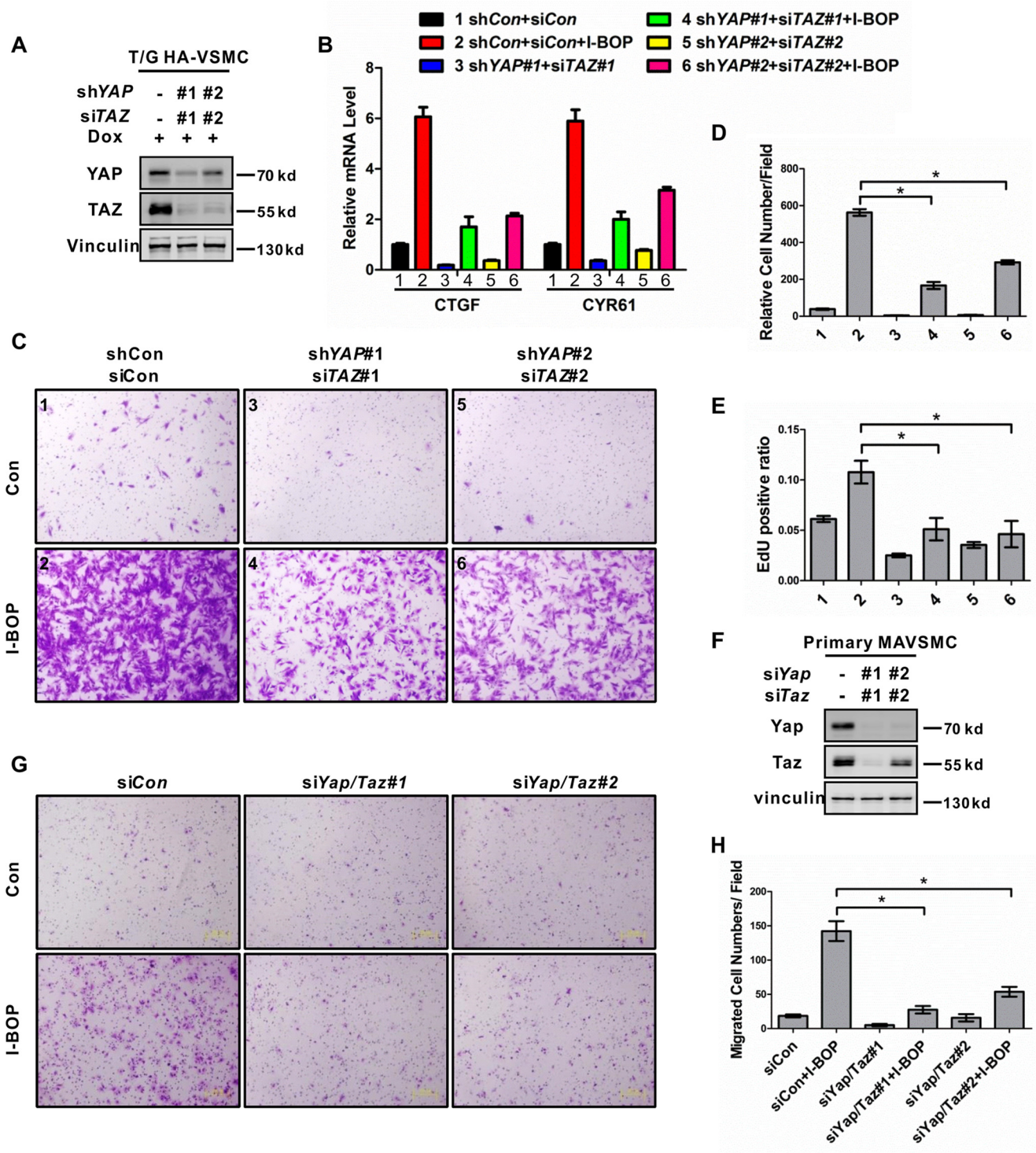

FIGURE 5. **YAP/TAZ mediate the effect of TP in gene induction, DNA synthesis, and cell migration in VSMCs.** *A*, knockdown of YAP/TAZ by shRNAs and siRNAs in T/G HA-VSMCs. Cells were transfected with the indicated siRNAs. 48 h after transfection and doxycycline (*Dox*) induction, cells were lysed and subjected to immunoblotting with the indicated antibodies. *B*, YAP/TAZ are required for I-BOP-induced gene expression. T/G HA-VSMCs were transfected with the indicated siRNAs and serum-starved for 24h in the presence of doxycycline. After treatment with I-BOP (1 nmol/liter) for 1 h, mRNA levels of CTGF and CYR61 were measured by real-time PCR. The numbers next to each treatment conditions will be used to label *C–E*. *C*, YAP/TAZ are required for I-BOP-induced cell migration. The treatment conditions for each panel are the same as in *B*. After stimulation with I-BOP (1 nmol/liter) for 4 h, cell migration was performed by transwell cell migration assay. Representative images are shown. *Con*, control. *D*, quantification result of the data in *C*. *, $p < 0.05$. Statistical analysis is described under "Experimental Procedures." *E*, YAP/TAZ are required for I-BOP-induced DNA synthesis. T/G HA-VSMCs were treated as indicated in *B* and then subjected to an EdU incorporation assay as described under "Experimental Procedures." About 600–1000 randomly selected cells are quantified and shown. *, $p < 0.05$. *F*, Yap/Taz knockdown by siRNAs in primary MAVSMCs. Cells were transfected with the indicated siRNAs. After 48-h transfection, cells were lysed and subjected to immunoblotting with the indicated antibodies. *G*, Yap/Taz are required for primary MAVSMCs migration induced by I-BOP. Primary MAVSMCs were transfected with the indicated siRNAs and serum-starved for 20 h. After stimulation with I-BOP (1 nmol/liter) for 4 h, cell migration was determined by transwell cell migration assay. Representative images are shown. *H*, quantification result of the data in *G*. *, $p < 0.05$.

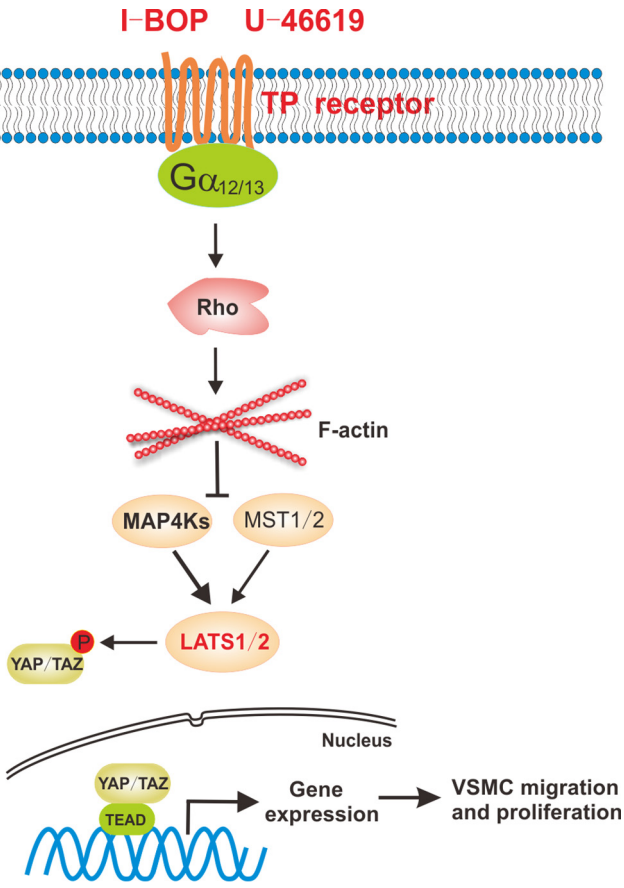

FIGURE 6. **A proposed model for thromboxane A2 receptor in the regulation of YAP/TAZ activities.**

mined by EdU incorporation (Fig. 5*E*, supplemental Fig. 8*A*). To further support the important role of the TP-YAP/TAZ axis in VSMCs, we isolated and analyzed primary MAVSMCs. Similar *Yap*/*Taz* knockdown experiments were performed in primary MAVSMCs. Consistently, knockdown of *Yap/Taz* in primary MAVSMCs also inhibited cell migration induced by I-BOP (Fig. 5, *F–H*). In addition, we observed that YAP/TAZ knockdown suppressed I-BOP-induced gene expression and cell migration in HeLa cells (supplemental Fig. 8, *B–D*). Taken together, these results demonstrate that YAP/TAZ play an important role in TP-mediated gene induction, cell proliferation, and migration in VSMCs.

Discussion

TxA2 is involved in multiple physiological and pathophysiological processes, including thrombosis, asthma, myocardial infarction, inflammation, atherosclerosis, and the response to vascular injury (11). TxA2 exerts its biological activity via its cognate TP receptor. In this study, we demonstrate that the Hippo pathway is a crucial downstream signaling module of TP receptor, a classical GPCR. TP agonists significantly activate YAP/TAZ in multiple cells lines, including VSMCs. Our data also demonstrate that activation of TP couples to $G\alpha_{12/13}$ to trigger the activation of Rho GTPase, which modulates the actin cytoskeleton to inhibit LATS1/2 kinase activity, resulting in YAP/TAZ dephosphorylation and activation (Fig. 6). In this signaling cascade, both MST1/2 and MAP4Ks, the major kinases for LATS1/2, are involved in Hippo pathway regulation by TP. Our studies indicate a functional role of the Hippo pathway and YAP/TAZ in mediating the physiological and pathological functions of thromboxane and its receptor TP.

In addition to TxA2, there are four other major prostaglandins generated from arachidonic acid *in vivo*, including prostaglandin D_2, prostaglandin E_2, prostaglandin $F_{2\alpha}$, and prostacyclin (48). They all exert their effects via corresponding GPCRs. It is interesting to speculate that YAP/TAZ may play a similar role in physiological and disease processes that are regulated by prostaglandins, such as inflammation, atherosclerosis, and cancer (49). For instance, the prostacyclin receptor couples to $G\alpha_s$ and stimulates cAMP production and PKA activation (50). Previously we reported that cAMP acts through PKA to stimulate LATS kinases and inhibit YAP (51). Given that TxA2 and prostacyclin are antagonistic in their actions in cardiovascular disease (6), it will be interesting to determine whether prostacyclin inhibits YAP/TAZ, thereby antagonizing the effect of TxA2, which activates YAP/TAZ, as shown in this report, in cardiovascular disease.

Isoprostanes are prostaglandin-like compounds formed from the free radical-catalyzed peroxidation of unsaturated fatty acids, such as arachidonic acid, that are recognized not only as reliable markers of oxidative stress but also as important mediators of various diseases (52). Increased formation of isoprostanes has been observed in diseases that are linked to oxidative stress, such as cardiovascular disease and cancer (52). As mentioned above, isoprostanes act, at least partially, via TP to exert their physiological effects. So one may speculate that YAP/TAZ also play a role in isoprostane-mediated pathophysiological effects. Indeed, we observed that 8-iso-prostaglandin $F_{2\alpha}$, a type of isoprostanes, could induce YAP/TAZ dephosphorylation in VSMCs.[5] Future studies are needed to delineate the involvement and potential role of YAP/TAZ in isoprostane-induced physiological processes.

Our study shows that YAP/TAZ are required for TP-stimulated VSMC DNA synthesis and cell migration. The connection between TP receptor and the Hippo pathway in vascular smooth muscle cells has important physiological implications. During vascular injury, activated platelets or other cells produce TxA2, which in turn promotes platelet activation and aggregation (4, 53). Besides TxA2, isoprostanes may also act through the TP receptor on the surface of smooth muscle cells and initiate the migration from media to intima via YAP/TAZ activation. Previous studies have reported that YAP is activated in VSMCs of the neointima (39). We propose that thromboxane acts through TP to induce YAP/TAZ activation to promote normal physiological wound healing in response to vascular injury. However, too much YAP/TAZ activation by TP under pathological conditions may lead to VSMC overgrowth, thereby contributing to neointima formation and restenosis. Notably, CTGF and CYR61 are strongly induced upon TP stimulation in a manner dependent on YAP/TAZ (Figs. 2*E* and 5*B*). Both CTGF and CYR61 have been shown to promote atherosclerotic lesion development and neointimal hyperplasia (54–

[5] X. Feng, P. Liu, X. Zhou, M. T. Li, F. L. Li, Z. Wang, Z. Meng, Y. P. Sun, Y. Yu, Y. Xiong, H. X. Yuan, and K. L. Guan, unpublished data.

56); therefore, uncontrolled expression of these proteins may contribute to pathology associated with TP hyperactivation. No TP antagonist has been used in clinics because of efficacy and toxicity issues (2). Our work reveals new insights into the role of the Hippo pathway and YAP/TAZ in thromboxane pathophysiology and suggests YAP/TAZ as potential therapeutic targets for vascular diseases. Actually, a small molecule, verteporfin (trade name Visudyne), a clinical drug for neovascular macular degeneration (57), has been shown to efficiently inhibit TEAD-YAP interaction and suppress YAP-induced liver overgrowth (58). The data in this report suggest that YAP/TAZ inhibitors could be a potential treatment for vascular diseases caused by VSMC overgrowth.

Experimental Procedures

Plasmids—The plasmids pCMV-HA-YAP2, FLAG-LATS1, FLAG-MST2, and FLAG-MAP4K2 and GFP-GDP dissociation inhibitor were described before (26, 51, 59). TPα/β were amplified from cDNA and then subcloned into pRK7-N-FLAG and pQCXIH vectors with the restriction enzymes BamHI/EcoRI.

Antibodies—Antibodies for YAP (4912), phospho-YAP (Ser-127, 4911), MST1 (3682), MST2 (3952), CYR61 (11952), phospho-MST1 (Thr-183)/MST2 (Thr-180, 3681), phospho-LATS1 (Ser-909, 9157), and phospho-LATS1 (Thr-1079, 8654) were purchased from Cell Signaling Technology. The LATS1 (A300-477A) and YAP (A302-308A) antibodies used for immunoprecipitation and LATS2 (A300-479A) antibody were from Bethyl Laboratories. TAZ (HPA007415) and Vinculin (V9264) antibodies were obtained from Sigma-Aldrich. Anti-TEAD1 (610922) was purchased from BD Transduction Laboratories. Antibodies for $G\alpha_{q/11}$ (Cys-19, sc-392) and $G\alpha_{12}$ (Ser-20, sc-409) and the HA-probe antibody (sc-7392) were from Santa Cruz Biotechnology. The tubulin antibody (581P) was purchased from NeoMarkers, and anti-β-actin (A00702), Lamin A/C (A01455), and anti-FLAG antibodies were purchased from GeneScript. The GFP tag (7G9, M20004) was from Abmart. The anti-G protein α_{13} antibody (EPR5436, ab128900) was obtained from Abcam.

Chemicals—U-46619 (9,11-dideoxy-9α,11α-methanoepoxy-prosta-5Z,13E-dien-1-oic acid) and SQ-29548 ([1S-[1α,2α(Z),3α,4α]]-7-[3-[[2-[(phenylamino)carbonyl]hydrazino]-methyl]-7-oxabicyclo[2.2.1]hept-2-yl]-5-heptenoic acid) were purchased from Santa Cruz Biotechnology. I-BOP ([1S-[1α,2α(Z),3β(1E,3S*),4 α]]-7-[3-[3-hydroxy-4-(4-iodophenoxy)-1-butenyl]-7-oxabicyclo[2.2.1]hept-2-yl]-5-heptenoic acid) was purchased from Cayman Chemical. Latrunculin B and tetramethylrhodamine B isothiocyanate-conjugated Phalloidin were purchased from Sigma-Aldrich. C3 was from Cytoskeleton Inc. Phos-tag was purchased from Wako chemicals. DAPI was purchased from Invitrogen.

Generation of Knockout Cells Using CRISPR/Cas9 Genome Editing—To generate TP knockout HEK293A cells, the following guide sequence targeting the human *TBXA2R* gene was used: 5′-GCTGGTGACCGGTACCATCG-3′. The detail protocol is described elsewhere (26). Two independent clones with *TBXA2R* gene deletion were used for experiments. MST1/2 dKO and LATS1/2 dKO HEK293A cells were described previously (26). MM-9KO HEK293A cells were generated based on MM-8KO cells (26). The following guide sequence targeting the human *MAP4K5* gene was used: 5′-CACCTAC-GGGGACGTCTATA-3′. Gene deletion was verified by Sanger sequencing of genomic DNA (supplemental Figs. S3 and S7).

Cell Culture—HEK239A and HeLa cells were cultured in DMEM (Invitrogen). U2OS cells were cultured in RPMI 1640 medium (Invitrogen). All of the above cells were supplemented with 10% FBS (Gibco) and 50 μg/ml penicillin/streptomycin. T/G HA-VSMCs were cultured in DMEM/F12 medium (Invitrogen) and supplemented with 0.05 mg/ml ascorbic acid, 0.01 mg/ml insulin, 0.01 mg/ml transferrin, 10 ng/ml sodium selenite, 0.03 mg/ml endothelial cell growth supplement, and 50 μg/ml penicillin/streptomycin. Mouse primary aortic VSMCs were isolated from 4- to 8-week-old C57BL/6 male mice using a standard protocol (60) and incubated in DMEM supplemented with 20% FBS and 50 μg/ml penicillin/streptomycin. Cells at passages 3–5 were used. For serum starvation, cells were incubated in DMEM or DMEM/F12 without serum. All cell lines were maintained at 37 °C with 5% CO_2.

Transfection and Lentiviral and Retroviral Infection—Cells were transfected with plasmid DNA using PEI. To generate U2OS cells stably expressing TPα/β, retroviruses carrying pQCXIH empty vector or pQCXIH-TPα/β were produced in HEK293T cells using vesicular stomatitis virus G and GAG as packaging plasmids. The virus supernatant was filtered through a 0.45-μm filter and used to infect targeting cells in the presence of 8 μg/ml Polybrene. Stable cell pools were selected with 50 μg/ml hygromycin B (Amresco) for 5 days. For tetracycline-inducible shRNA expression, a lentivirus containing shRNAs in the pTRIPZ vector was made in HEK293T cells using pMD2.g and psPAX2 as packaging plasmids. Virus infection was performed as described above except for selection with 1 μg/ml puromycin (Amresco) for 5 days. Expression of shRNA was induced by adding 1 μg/ml doxycycline for 48 h. The shRNA sequences against YAP were as follows: YAP#1, TTCTTTATCT-AGCTTGGTGGC; YAP#2, TGGTCAGAGATACTTCTTAAA.

RNA Interference—siRNAs targeting *GNAQ*, *GNA11*, *GNA12*, *GNA13*, *YAP1/Yap1*, and *WWTR1/Wwtr1* were from Genepharma and were delivered into cells using RNAiMAX (Invitrogen) according to the instructions of the manufacturer. The sequences of all siRNAs used in this study were as follows: si*GNAQ* #1, GACACCGAGAATATCCGCTTT; si*GNAQ* #2, CTAT-GATAGACGACGAGAATA; si*GNA11* #1, GCTCAAGATC-CTCTACAAGTA; si*GNA11*#2, GCTCAACCTCAAGGAGTA-CAA; si*GNA12*#1, GCGACACCATCTTCGACAA; si*GNA12*#2, GGATGTTCCTGATGGCCTT; si*GNA13*#1, GCTCGAGAG-AAGCTTCATA; si*GNA13*#2, CCTGCTATAAGAGCATTAT; si*YAP1*#1, CCCAGTTAAATGTTCACCAAT; si*YAP1*#2, CAG-GTGATACTATCAACCAAA; si*TAZ*#1, CAGCCAAAT-CTCGTGATGAAT; si*TAZ*#2, GCGATGAATCAGCCTCT-GAAT; si*Yap1*#1, GAAGCGCTGAGTTCCGAAATC; si*Yap1*#2, TGAGAACAATGACAACCAATA; si*Taz*#1, CAGCCGAAT-CTCGCAATGAAT; and si*Taz*#2, CCATGAGCACAGATAT-GAGAT.

RNA Extraction and Real-time PCR—Cells were washed with cold PBS, and total RNA was isolated using TRIzol reagent following the instructions of the manufacturer (Invitrogen). 1 μg of RNA was reverse-transcribed to cDNA with oligo(dT) prim-

ers (Transgene). cDNA was then diluted and subjected to real-time PCR with gene-specific primers using SYBR Premix Ex Taq (TaKaRa) and the 7500 real-time PCR system (Applied Biosystems). The primer pairs used in this study were as follows: Actin, GCCGACAGGATGCAGAAGGAGATCA/AAGCATTTGCGGTGGACGATGGA; CTGF, CCAATGACAACGCCTCCTG/TGGTGCAGCCAGAAAGCTC; CYR61, AGCCTCGCATCCTATACAACC/TTCTTTCACAAGGCGGCACTC; EDN1, TGTGTCTACTTCTGCCACCT/CCCTGAGTTCTTTTCCTGCTT; ANKRD1, CACTTCTAGCCCACCCTGTGA/CCACAGGTTCCGTAATGATTT; TAGLN, CCCGAGAACCCACCCTCCA/AAAGCCATCAGGGTCCTCTGC; TPα, CCTTCTGGTCTTCATCGCCC/CTGGAGGGACAGCGACCT; and TPβ, ACCCGGCCCAGACGGAGT/GGACAGAGCCTTCCCTGTTGG.

Immunoprecipitation—Cells were lysed using lysis buffer (50 mM Tris (pH 7.5), 150 mM NaCl, 0.5% Nonidet P-40, 50 mM NaF, 1.5 mM Na_3VO_4, 1 mM PMSF, and protease inhibitors). Cell lysates were centrifuged at 12,000 $\times$ *g* for 15 min at 4 °C. The supernatants were incubated with YAP antibody (Bethyl Laboratories) for 2 h, followed by protein A-agarose bead incubation for 1 h. Immunoprecipitates were washed three times with lysis buffer, and proteins were boiled with SDS-PAGE sample buffer.

Immunoblotting—Cells were lysed in SDS sample buffer and denatured by heating on 99 °C for 10 min. Immunoblotting was performed in 8% or 10% BisTris polyacrylamide gel according to the standard protocol. The phos-tag reagents were purchased from Wako Chemicals, and gels containing phos-tag were prepared following the instructions of the manufacturer. YAP and TAZ proteins can be separated into multiple bands in phos-tag gels depending on differential phosphorylation levels, with phosphorylated YAP/TAZ migrating more slowly.

Immunofluorescence Staining—Cells seeded in 6-well plates were treated as indicated in specific experiments. After treatment, they were fixed immediately with 4% paraformaldehyde for 20 min and then permeabilized with 0.5% Triton X-100 in PBS for 5 min on ice. After blocking in 5% BSA for 30 min, cells were incubated with primary antibodies overnight at 4 °C. Cells were washed with PBS three times for 5 min, and Alexa Fluor 488-conjugated secondary antibodies were added for 1 h at room temperature. Tetramethylrhodamine B isothiocyanate-conjugated Phalloidin was used to stain actin filaments, and DAPI was used for cell nuclei. Photos were taken by an Olympus IX81 inverted research microscope with appropriate fluorescence filters.

Cell Fractionation—HeLa cells were seeded with a density of 6×10^4 cells/cm^2 for 12 h, starved in serum-free medium for 16 h, and stimulated with 1 nmol/liter I-BOP or 10 nmol/liter U-46619 for 1 h. Subcellular fractionation was performed with NE-PER^{TM} nuclear and cytoplasmic extraction reagent (Thermo Fisher) according to the instructions of the manufacturer. Both fractions were analyzed by Western blotting.

In Vitro Kinase Assay—LATS1 kinase assay was performed as described before (38). Briefly, LATS1 was immunoprecipitated from cells and subjected to an *in vitro* kinase assay using GST-YAP as a substrate. The phosphorylation levels of GST-YAP at Ser-127 were determined by immunoblotting using phospho-YAP (Ser-127) antibody.

Transwell Migration Assay—Cell migration assays were performed using BD Falcon Cell culture inserts for 24-well plates with 8.0-μm pore filters. Cells were serum-starved for 20 h and then stimulated with I-BOP or vehicle for 4 h. Cells (6×10^4 T/G HA-VSMCs, 5×10^4 primary aortic VSMCs, and 2×10^5 HeLa cells) were seeded into the upper chamber of the insert for each well in DMEM/F-12 without other supplements, and the lower chamber of the plate was filled with DMEM/F-12 supplemented with 10% FBS. After 6 h for T/G HA-VSMC (3 h for primary MAVSMC and 24 h for HeLa), cells were fixed using 4% paraformaldehyde and stained with 0.05% crystal violet. Cells in the upper chamber were removed by scrubbing with a cotton swab, and cells migrated through the filter were photographed and quantified.

EdU Incorporation Assay—T/G HA-VSMCs grown on 24-well plates were serum-starved for 24 h. I-BOP (1 nmol/liter) was added every 8 h for 3 times. 10 μmol/liter EdU (5-ethynyl-2′-deoxyuridine) was added to the culture medium for 4 h. After labeling, cells were fixed with 4% paraformaldehyde for 20 min, followed by permeabilization with 0.5% Triton X-100 in PBS for 20 min at room temperature. Cells were rinsed once with PBS and incubated with mixture reaction buffer (100 mmol/liter sodium ascorbate, 4.8 μmol/liter Alexa Fluor 488 azide, and 4 mmol/liter $CuSO_4$) for 30 min at room temperature. After staining, cells were washed three times with 0.5% Triton X-100 in PBS, and DAPI was used for cell nuclei. Photos were taken by an Olympus IX81 inverted research microscope.

Statistical Analysis—All data are expressed as mean ± S.E. Two-group comparison was analyzed by Student's *t* test. $p < 0.05$ was considered significant.

Author Contributions—X. F., Y. X., H. X. Y., and K. L. G designed the research, analyzed the data, and wrote the manuscript. X. F. performed the experiments with assistance from P. L., X. Z., M. T. L, F. L. L, Z. W., Z. P. M., and Y. P. S. Y. Y. provided technical and intellectual support. All authors discussed the results and commented on the manuscript.

Acknowledgments—We thank Dan Ye and the members of the Fudan MCB laboratory for support throughout the course of this study.

References

1. Hamberg, M., Svensson, J., and Samuelsson, B. (1975) Thromboxanes: a new group of biologically active compounds derived from prostaglandin endoperoxides. *Proc. Natl. Acad. Sci. U.S.A.* **72,** 2994–2998
2. Ting, H. J., Murad, J. P., Espinosa, E. V., and Khasawneh, F. T. (2012) Thromboxane A2 receptor: biology and function of a peculiar receptor that remains resistant for therapeutic targeting. *J. Cardiovasc. Pharmacol. Ther.* **17,** 248–259
3. Braden, G. A., Knapp, H. R., and FitzGerald, G. A. (1991) Suppression of eicosanoid biosynthesis during coronary angioplasty by fish oil and aspirin. *Circulation* **84,** 679–685
4. Byrne, A., Moran, N., Maher, M., Walsh, N., Crean, P., and Fitzgerald, D. J. (1997) Continued thromboxane A2 formation despite administration of a platelet glycoprotein IIb/IIIa antagonist in patients undergoing coronary angioplasty. *Arterioscler. Thromb. Vasc. Biol.* **17,** 3224–3229
5. Belton, O., Byrne, D., Kearney, D., Leahy, A., and Fitzgerald, D. J. (2000)

Cyclooxygenase-1 and -2-dependent prostacyclin formation in patients with atherosclerosis. *Circulation* **102,** 840–845
6. Cheng, Y., Austin, S. C., Rocca, B., Koller, B. H., Coffman, T. M., Grosser, T., Lawson, J. A., and FitzGerald, G. A. (2002) Role of prostacyclin in the cardiovascular response to thromboxane A2. *Science* **296,** 539–541
7. Belton, O. A., Duffy, A., Toomey, S., and Fitzgerald, D. J. (2003) Cyclooxygenase isoforms and platelet vessel wall interactions in the apolipoprotein E knockout mouse model of atherosclerosis. *Circulation* **108,** 3017–3023
8. Praticò, D., Cyrus, T., Li, H., and FitzGerald, G. A. (2000) Endogenous biosynthesis of thromboxane and prostacyclin in 2 distinct murine models of atherosclerosis. *Blood* **96,** 3823–3826
9. Yamagami, S., Miyauchi, K., Kimura, T., Goh, Y., Daida, H., and Yamaguchi, H. (1999) Effects of the thromboxane A2 receptor antagonist on platelet deposition and intimal hyperplasia after balloon injury. *Jpn. Heart J.* **40,** 791–802
10. Inoue, T., and Node, K. (2009) Molecular basis of restenosis and novel issues of drug-eluting stents. *Circ. J.* **73,** 615–621
11. Nakahata, N. (2008) Thromboxane A2: physiology/pathophysiology, cellular signal transduction and pharmacology. *Pharmacol. Ther.* **118,** 18–35
12. Montuschi, P., Barnes, P. J., and Roberts, L. J., 2nd. (2004) Isoprostanes: markers and mediators of oxidative stress. *FASEB J.* **18,** 1791–1800
13. Gluais, P., Lonchampt, M., Morrow, J. D., Vanhoutte, P. M., and Feletou, M. (2005) Acetylcholine-induced endothelium-dependent contractions in the SHR aorta: the Janus face of prostacyclin. *Br. J. Pharmacol.* **146,** 834–845
14. Audoly, L. P., Rocca, B., Fabre, J. E., Koller, B. H., Thomas, D., Loeb, A. L., Coffman, T. M., and FitzGerald, G. A. (2000) Cardiovascular responses to the isoprostanes iPF(2α)-III and iPE(2)-III are mediated via the thromboxane A(2) receptor *in vivo*. *Circulation* **101,** 2833–2840
15. Ishimitsu, T., Uehara, Y., Ishii, M., Ikeda, T., Matsuoka, H., and Sugimoto, T. (1988) Thromboxane and vascular smooth muscle cell growth in genetically hypertensive rats. *Hypertension* **12,** 46–51
16. Ishimitsu, T., Uehara, Y., Ishii, M., and Sugimoto, T. (1988) Enhanced generation of vascular thromboxane A2 in spontaneously hypertensive rats and its role in the rapid proliferation of vascular smooth muscle cells. *Am. J. Hypertens.* **1,** 38S–40S
17. Hanasaki, K., Nakano, T., and Arita, H. (1990) Receptor-mediated mitogenic effect of thromboxane A2 in vascular smooth muscle cells. *Biochem. Pharmacol.* **40,** 2535–2542
18. Pakala, R., Willerson, J. T., and Benedict, C. R. (1997) Effect of serotonin, thromboxane A2, and specific receptor antagonists on vascular smooth muscle cell proliferation. *Circulation* **96,** 2280–2286
19. Pakala, R. (2004) Serotonin and thromboxane A2 stimulate platelet-derived microparticle-induced smooth muscle cell proliferation. *Cardiovasc. Radiat. Med.* **5,** 20–26
20. Yokota, T., Shiraishi, R., Aida, T., Iwai, K., Liu, N. M., Yokoyama, U., and Minamisawa, S. (2014) Thromboxane A(2) receptor stimulation promotes closure of the rat ductus arteriosus through enhancing neointima formation. *PLoS ONE* **9,** e94895
21. Owens, G. K., Kumar, M. S., and Wamhoff, B. R. (2004) Molecular regulation of vascular smooth muscle cell differentiation in development and disease. *Physiol. Rev.* **84,** 767–801
22. Cayatte, A. J., Du, Y., Oliver-Krasinski, J., Lavielle, G., Verbeuren, T. J., and Cohen, R. A. (2000) The thromboxane receptor antagonist S18886 but not aspirin inhibits atherogenesis in apo E-deficient mice: evidence that eicosanoids other than thromboxane contribute to atherosclerosis. *Arterioscler. Thromb. Vasc. Biol.* **20,** 1724–1728
23. Kobayashi, T., Tahara, Y., Matsumoto, M., Iguchi, M., Sano, H., Murayama, T., Arai, H., Oida, H., Yurugi-Kobayashi, T., Yamashita, J. K., Katagiri, H., Majima, M., Yokode, M., Kita, T., and Narumiya, S. (2004) Roles of thromboxane A(2) and prostacyclin in the development of atherosclerosis in apoE-deficient mice. *J. Clin. Invest.* **114,** 784–794
24. Egan, K. M., Wang, M., Fries, S., Lucitt, M. B., Zukas, A. M., Puré, E., Lawson, J. A., and FitzGerald, G. A. (2005) Cyclooxygenases, thromboxane, and atherosclerosis: plaque destabilization by cyclooxygenase-2 inhibition combined with thromboxane receptor antagonism. *Circulation* **111,** 334–342
25. Yu, F. X., Zhao, B., and Guan, K. L. (2015) Hippo pathway in organ size control, tissue homeostasis, and cancer. *Cell* **163,** 811–828
26. Meng, Z., Moroishi, T., Mottier-Pavie, V., Plouffe, S. W., Hansen, C. G., Hong, A. W., Park, H. W., Mo, J.-S., Lu, W., Lu, S., Flores, F., Yu, F.-X., Halder, G., and Guan, K.-L. (2015) MAP4K family kinases act in parallel to MST1/2 to activate LATS1/2 in the Hippo pathway. *Nat. Commun.* **6,** 8357
27. Zheng, Y., Wang, W., Liu, B., Deng, H., Uster, E., and Pan, D. (2015) Identification of Happyhour/MAP4K as alternative Hpo/Mst-like kinases in the Hippo kinase cascade. *Dev. Cell* **34,** 642–655
28. Dong, J., Feldmann, G., Huang, J., Wu, S., Zhang, N., Comerford, S. A., Gayyed, M. F., Anders, R. A., Maitra, A., and Pan, D. (2007) Elucidation of a universal size-control mechanism in *Drosophila* and mammals. *Cell* **130,** 1120–1133
29. Zhao, B., Wei, X., Li, W., Udan, R. S., Yang, Q., Kim, J., Xie, J., Ikenoue, T., Yu, J., Li, L., Zheng, P., Ye, K., Chinnaiyan, A., Halder, G., Lai, Z. C., and Guan, K. L. (2007) Inactivation of YAP oncoprotein by the Hippo pathway is involved in cell contact inhibition and tissue growth control. *Genes Dev.* **21,** 2747–2761
30. Lei, Q. Y., Zhang, H., Zhao, B., Zha, Z. Y., Bai, F., Pei, X. H., Zhao, S., Xiong, Y., and Guan, K. L. (2008) TAZ promotes cell proliferation and epithelial-mesenchymal transition and is inhibited by the Hippo pathway. *Mol. Cell. Biol.* **28,** 2426–2436
31. Zhao, B., Ye, X., Yu, J., Li, L., Li, W., Li, S., Yu, J., Lin, J. D., Wang, C. Y., Chinnaiyan, A. M., Lai, Z. C., and Guan, K. L. (2008) TEAD mediates YAP-dependent gene induction and growth control. *Genes Dev.* **22,** 1962–1971
32. Zhao, B., Li, L., Tumaneng, K., Wang, C. Y., and Guan, K. L. (2010) A coordinated phosphorylation by Lats and CK1 regulates YAP stability through SCF β-TRCP. *Genes Dev.* **24,** 72–85
33. Harvey, K. F., Zhang, X., and Thomas, D. M. (2013) The Hippo pathway and human cancer. *Nat. Rev. Cancer* **13,** 246–257
34. Miller, E., Yang, J., DeRan, M., Wu, C., Su, A. I., Bonamy, G. M., Liu, J., Peters, E. C., and Wu, X. (2012) Identification of serum-derived sphingosine-1-phosphate as a small molecule regulator of YAP. *Chem. Biol.* **19,** 955–962
35. Mo, J. S., Yu, F. X., Gong, R., Brown, J. H., and Guan, K. L. (2012) Regulation of the Hippo-YAP pathway by protease-activated receptors (PARs). *Genes Dev.* **26,** 2138–2143
36. Yu, F. X., Zhao, B., Panupinthu, N., Jewell, J. L., Lian, I., Wang, L. H., Zhao, J., Yuan, H., Tumaneng, K., Li, H., Fu, X. D., Mills, G. B., and Guan, K. L. (2012) Regulation of the Hippo-YAP pathway by G-protein-coupled receptor signaling. *Cell* **150,** 780–791
37. Wennmann, D. O., Vollenbröker, B., Eckart, A. K., Bonse, J., Erdmann, F., Wolters, D. A., Schenk, L. K., Schulze, U., Kremerskothen, J., Weide, T., and Pavenstädt, H. (2014) The Hippo pathway is controlled by angiotensin II signaling and its reactivation induces apoptosis in podocytes. *Cell Death Dis.* **5,** e1519
38. Zhou, X., Wang, S., Wang, Z., Feng, X., Liu, P., Lv, X. B., Li, F., Yu, F. X., Sun, Y., Yuan, H., Zhu, H., Xiong, Y., Lei, Q. Y., and Guan, K. L. (2015) Estrogen regulates Hippo signaling via GPER in breast cancer. *J. Clin. Invest.* **125,** 2123–2135
39. Wang, X., Hu, G., Gao, X., Wang, Y., Zhang, W., Harmon, E. Y., Zhi, X., Xu, Z., Lennartz, M. R., Barroso, M., Trebak, M., Chen, C., and Zhou, J. (2012) The induction of yes-associated protein expression after arterial injury is crucial for smooth muscle phenotypic modulation and neointima formation. *Arterioscler. Thromb. Vasc. Biol.* **32,** 2662–2669
40. Xie, C., Guo, Y., Zhu, T., Zhang, J., Ma, P. X., and Chen, Y. E. (2012) Yap1 protein regulates vascular smooth muscle cell phenotypic switch by interaction with myocardin. *J. Biol. Chem.* **287,** 14598–14605
41. Dupont, S., Morsut, L., Aragona, M., Enzo, E., Giulitti, S., Cordenonsi, M., Zanconato, F., Le Digabel, J., Forcato, M., Bicciato, S., Elvassore, N., and Piccolo, S. (2011) Role of YAP/TAZ in mechanotransduction. *Nature* **474,** 179–183
42. Fernández, B. G., Gaspar, P., Brás-Pereira, C., Jezowska, B., Rebelo, S. R., and Janody, F. (2011) Actin-capping protein and the Hippo pathway regulate F-actin and tissue growth in *Drosophila*. *Development* **138,** 2337–2346

43. Rauskolb, C., Pan, G., Reddy, B. V., Oh, H., and Irvine, K. D. (2011) Zyxin links fat signaling to the hippo pathway. *PLoS Biol.* **9,** e1000624
44. Sansores-Garcia, L., Bossuyt, W., Wada, K., Yonemura, S., Tao, C., Sasaki, H., and Halder, G. (2011) Modulating F-actin organization induces organ growth by affecting the Hippo pathway. *EMBO J.* **30,** 2325–2335
45. Zhao, B., Li, L., Wang, L., Wang, C. Y., Yu, J., and Guan, K. L. (2012) Cell detachment activates the Hippo pathway via cytoskeleton reorganization to induce anoikis. *Genes Dev.* **26,** 54–68
46. Chan, E. H., Nousiainen, M., Chalamalasetty, R. B., Schäfer, A., Nigg, E. A., and Silljé, H. H. (2005) The Ste20-like kinase Mst2 activates the human large tumor suppressor kinase Lats1. *Oncogene* **24,** 2076–2086
47. Marx, S. O., Totary-Jain, H., and Marks, A. R. (2011) Vascular smooth muscle cell proliferation in restenosis. *Circ. Cardiovasc. Interv.* **4,** 104–111
48. Ricciotti, E., and FitzGerald, G. A. (2011) Prostaglandins and inflammation. *Arterioscler. Thromb. Vasc. Biol.* **31,** 986–1000
49. Smyth, E. M., Grosser, T., Wang, M., Yu, Y., and FitzGerald, G. A. (2009) Prostanoids in health and disease. *J. Lipid Res.* **50,** S423–S428
50. Fetalvero, K. M., Shyu, M., Nomikos, A. P., Chiu, Y. F., Wagner, R. J., Powell, R. J., Hwa, J., and Martin, K. A. (2006) The prostacyclin receptor induces human vascular smooth muscle cell differentiation via the protein kinase A pathway. *Am. J. Physiol. Heart Circ. Physiol.* **290,** H1337–H1346
51. Yu, F. X., Zhang, Y., Park, H. W., Jewell, J. L., Chen, Q., Deng, Y., Pan, D., Taylor, S. S., Lai, Z. C., and Guan, K. L. (2013) Protein kinase A activates the Hippo pathway to modulate cell proliferation and differentiation. *Genes Dev.* **27,** 1223–1232
52. Bauer, J., Ripperger, A., Frantz, S., Ergün, S., Schwedhelm, E., and Benndorf, R. A. (2014) Pathophysiology of isoprostanes in the cardiovascular system: implications of isoprostane-mediated thromboxane A2 receptor activation. *Br. J. Pharmacol.* **171,** 3115–3131
53. Peterson, M. B., Machaj, V., Block, P. C., Palacios, I., Philbin, D., and Watkins, W. D. (1986) Thromboxane release during percutaneous transluminal coronary angioplasty. *Am. Heart J.* **111,** 1–6
54. Cicha, I., Yilmaz, A., Klein, M., Raithel, D., Brigstock, D. R., Daniel, W. G., Goppelt-Struebe, M., and Garlichs, C. D. (2005) Connective tissue growth factor is overexpressed in complicated atherosclerotic plaques and induces mononuclear cell chemotaxis *in vitro*. *Arterioscler. Thromb. Vasc. Biol.* **25,** 1008–1013
55. Matsumae, H., Yoshida, Y., Ono, K., Togi, K., Inoue, K., Furukawa, Y., Nakashima, Y., Kojima, Y., Nobuyoshi, M., Kita, T., and Tanaka, M. (2008) CCN1 knockdown suppresses neointimal hyperplasia in a rat artery balloon injury model. *Arterioscler. Thromb. Vasc. Biol.* **28,** 1077–1083
56. Lee, H. Y., Chung, J. W., Youn, S. W., Kim, J. Y., Park, K. W., Koo, B. K., Oh, B. H., Park, Y. B., Chaqour, B., Walsh, K., and Kim, H. S. (2007) Forkhead transcription factor FOXO3a is a negative regulator of angiogenic immediate early gene CYR61, leading to inhibition of vascular smooth muscle cell proliferation and neointimal hyperplasia. *Circ. Res.* **100,** 372–380
57. Michels, S., and Schmidt-Erfurth, U. (2001) Photodynamic therapy with verteporfin: a new treatment in ophthalmology. *Semin. Ophthalmol.* **16,** 201–206
58. Liu-Chittenden, Y., Huang, B., Shim, J. S., Chen, Q., Lee, S. J., Anders, R. A., Liu, J. O., and Pan, D. (2012) Genetic and pharmacological disruption of the TEAD-YAP complex suppresses the oncogenic activity of YAP. *Genes Dev.* **26,** 1300–1305
59. Lv, X. B., Liu, C. Y., Wang, Z., Sun, Y. P., Xiong, Y., Lei, Q. Y., and Guan, K. L. (2015) PARD3 induces TAZ activation and cell growth by promoting LATS1 and PP1 interaction. *EMBO Rep.* **16,** 975–985
60. Ray, J. L., Leach, R., Herbert, J. M., and Benson, M. (2001) Isolation of vascular smooth muscle cells from a single murine aorta. *Methods Cell Sci.* **23,** 185–188